Development of a Transportable Quantum Gravity Gradiometer for Gravity Field Mapping

James M. Kohel, Robert J. Thompson, James R. Kellogg, David C. Aveline, and Nan Yu
Jet Propulsion Laboratory, California Institute of Technology
4800 Oak Grove Drive
Pasadena, California 91109-8099

Abstract – **We are developing a transportable gravity gradiometer based on atom-wave interferometry for NASA's Earth Science Technology Office Instrument Incubator Program. Atom interferometry is an enabling technology that employs a matter-wave interference measurement with individual atoms as proof masses for inertial sensing. A laboratory version of this instrument has been recently demonstrated, and the current effort is to further the maturity of this technology by developing a transportable instrument for measurements in the field. This is an important developmental step towards a new class of space-borne instruments which can contribute to NASA's global gravity field mapping and monitoring efforts. In this paper, we will briefly review the principles and technology of atom interferometer-based inertial sensors, then describe the technical implementation and status of the transportable instrument.**

I. Introduction

The detection of the quantum interference of atomic states is a particularly versatile metrology tool, allowing precision measurements of a wide variety of physical phenomena. For the past sixty years, atomic clocks employing quantum interference measurements have evolved into remarkably precise laboratory instruments (keeping track of one second in a billion years), and have been widely implemented in a variety of demanding real-world applications (GPS atomic clocks, for example, are capable of operating for years in a space environment). The sensitivity of this quantum interference technique in inertial sensors has already been demonstrated in the laboratory [1–6], and there is great interest in applying this technique to gravity mapping studies from space.

This technology is of particular importance to NASA for two reasons. First, gravity field mapping is one of the key measurements required in order to understand the solid earth, ice and oceans, and dynamic processes in a comprehensive model of our planet. There have been a number of gravity measurement missions, such as CHAMP [7] and GRACE [8], which measure gravity through the precise monitoring of the relative motion of satellites or onboard drag-free test masses, and other gravity missions using mechanical gravity gradiometers have also been planned or are under development [9,10]. Secondly, the microgravity environment of space promises a significant enhancement of the inertial sensing performance of an atom interferometer based on cold atoms.

In this paper we will discuss the design and implementation of a next generation prototype being developed as part of the NASA's Instrument Incubator Program (IIP). This instrument will be capable of mounting on a mobile platform, so as to make measurements in remote locations. Building on extensive experience at JPL with atomic clock technology, we aim to produce a practical instrument that fully realizes the power of quantum interference to measure the local gravity field.

II. Principles of Operation

The quantum gravity gradiometer employs two cold atom interferometers using laser-induced stimulated Raman transitions [11,12] to measure differential accelerations along the vertical direction. The atom interferometers are realized by using a $\pi/2$–π–$\pi/2$ laser pulse sequence to drive velocity-sensitive stimulated Raman transitions between the two ground hyperfine states in cesium atoms in both interferometers. The counter-propagating Raman laser beams are oriented along the vertical launch axis, parallel to the direction of gravitational acceleration to be measured. The first $\pi/2$ pulse at time t_1 creates an equal superposition of atoms in the two hyperfine ground states. Only the excited state receives a photon recoil kick and therefore travels at a slightly different velocity, realizing a beam splitting analogous to that in a traditional Mach-Zehnder interferometer. Subsequent π and $\pi/2$ pulses at times $t_2 = t_1+T$ and $t_3 = t_1+2T$, respectively, similarly redirect and recombine the atom waves to complete an interferometer loop, as illustrated in Fig. 1. The transition probability resulting from this interferometer sequence is given by $P = \frac{1}{2}[1 - \cos(\Delta\phi)]$, where $\Delta\phi$ is the net phase difference between the two interferometer paths. This phase difference can be calculated from the Raman laser phases at the time and location of each interaction, *i.e.* $\Delta\phi = \phi(t_1, z_1) - 2\phi(t_2, z_2) + \phi(t_3, z_3)$. The phase shift $\Delta\phi$ is related to the acceleration $\mathbf{a}$ according to $\Delta\phi = \mathbf{k}_{\text{eff}} \cdot \mathbf{a}T^2$, where T is the time between pulses and $\mathbf{k_{eff}} \equiv \mathbf{k_1} - \mathbf{k_2} \approx 2\mathbf{k_1}$ is the effective Raman laser wave number. The acceleration $\mathbf{a}$ is a vector sum of the gravitational acceleration g and platform acceleration a_p.

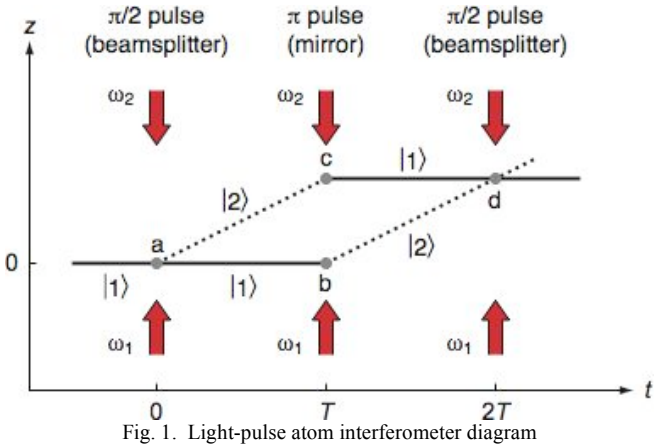

Fig. 1. Light-pulse atom interferometer diagram

The atom interferometer phase shift can be measured by detecting the relative populations of the two hyperfine ground states via laser-induced fluorescence. The observed normalized signal takes the form of $P(\Delta\phi) = P_{\min} + \frac{1}{2}A[1 - \cos(\phi_0 + \Delta\phi)]$, where A is the normalized fringe amplitude $P_{max} - P_{min}$. To illustrate the sensitivity of a single such interferometer, consider a measurement with interrogation time $2T = 1$ s. As little as $3 \times 10^{-8}g$ of acceleration will cause a fringe phase shift of one full radian, and the acceleration measurement sensitivity will be determined by the SNR in the fringe measurement. A recent laboratory measurement demonstrated a resolution of $3 \times 10^{-9}g$ after 60 s and $1 \times 10^{-10}g$ after two days integration time [2].

Although the gravitational acceleration can be measured directly as described above, this measurement requires an inertial frame of reference (*i.e.* $a_p = 0$). This is a consequence of Einstein's Equivalence Principle: *i.e.* that an acceleration of the reference frame is indistinguishable from the gravitational acceleration in a local measurement. An inertial frame is difficult to realize, even in a laboratory environment. Gravity gradiometry thus provides a more fundamental measure of the gravitational fields by measuring the gravitational acceleration difference between two locations using a common reference frame so that other non-inertial accelerations are rejected as common-mode noise. In the quantum gravity gradiometer, the two acceleration measurements are performed simultaneously in two atom interferometers separated by a distance d by using the same Raman laser beams. Platform vibrations and laser fluctuations are effectively cancelled in the differential measurement [5], so the phase shift gives the gravitational acceleration difference in the two locations, and the linear gravity gradient can be derived from the baseline distance d. With this configuration, a differential acceleration sensitivity of $4 \times 10^{-9}g$ $\mathrm{Hz}^{-1/2}$ has been demonstrated in our laboratory prototype [6]. With the measurement baseline of 1.4 m in this instrument, this corresponds to a gravity gradient sensitivity of 34 E $\mathrm{Hz}^{-1/2}$ (1 E $\equiv 10^{-9}$ s^{-2}).

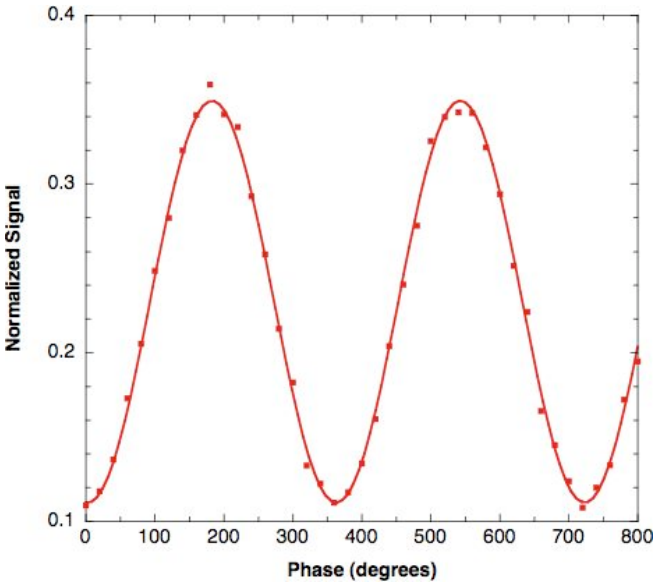

Fig. 2. Atom interferometer fringes as observed in our laboratory prototype instrument [6]. The phase of the final Raman π/2 pulse was scanned to generate the characteristic interferometer fringe.

A. Microgravity operation

In general, precision measurements employing ultra-cold atoms are dramatically improved in microgravity due to the longer interaction times available. For the gradiometer this enhancement is much more profound, as the measurement sensitivity increases with the *square* of the interrogation time, in contrast to the linear dependence for Fourier-transform-limited measurements in atomic clocks. In a ground-based experiment in an atomic fountain, for example, the interrogation time is limited to a fraction of a second due to practical limitations in the physical height of the apparatus. In a microgravity environment, however, interrogation times are limited only by the slow thermal expansion of the laser-cooled atoms. The benefits of microgravity operation has been recognized in other experiments with cold atom clocks [13,14]. Experiments using cold atom interferometers in space have already been proposed to perform fundamental tests of Einstein's General Relativity and the Equivalence Principle [15].

III. Instrument Development

Our next-generation gravity gradiometer is designed as a transportable instrument capable of operating outside the laboratory environment. Such an instrument must be capable of unattended operation in a remote location, and is subject to significant design constraints in order to accommodate the additional requirements of size, weight, power consumption, environmental control and robustness for a transportable instrument. The current instrument is intended to operate while stationary in the field (an additional stabilized platform would be necessary to take data from a mov-

ing platform), and as a terrestrial instrument, it differs by design from a gravity gradiometer intended for microgravity operation. Despite these differences, the current effort is a significant step in advancing the technology along the development path toward future space-based instruments.

A. Atomic physics package

The current gravity gradiometer consists of two atom interferometer-based accelerometers housed in a single ultra-high vacuum (UHV) enclosure which is the main component of the atomic physics package. The two interferometers are separated by 1 m in the vertical direction. Each accelerometer operates in an atomic fountain configuration. The UHV enclosure incorporates two titanium chambers with welded sapphire windows (Fig. 3). The chambers are connected by a titanium tube, and the UHV condition is maintained by a non-evaporable getter (NEG) pump and an ion pump located along this tube between the individual chambers. The ion pump is necessary only due to the presence of residual argon, which we attribute to the presence of virtual leaks in the TIG-welded sections of the titanium chamber. The outgas rate for this argon was measured at less than 1×10^{-10} Torr l/s, and has remained constant over several months of operation. After the initial bakeout at 250 C, we obtained a total background pressure less than 1×10^{-10} Torr in the UHV chamber.

Fig. 3. Close-up of hexagonal titanium chamber with welded sapphire windows and magnetic coils, with laser collimators removed.

In order to operate the two atom fountains under these UHV conditions, we have developed separate 2D-MOTs which provide a cold atom beam source for loading each UHV MOT [16]. Each compact 2D-MOT source operates in a $19 \times 19 \times 64$ mm^3 glass cell. The glass cells contain cesium vapor at a pressure between $5–7 \times 10^{-7}$ Torr, and the pressure differential between the vapor cell source regions and the UHV science region is maintained by a graphite-lined differential-pumping tube. The UHV MOTs and the 2D-MOT beam sources with optics are shown in Fig. 4.

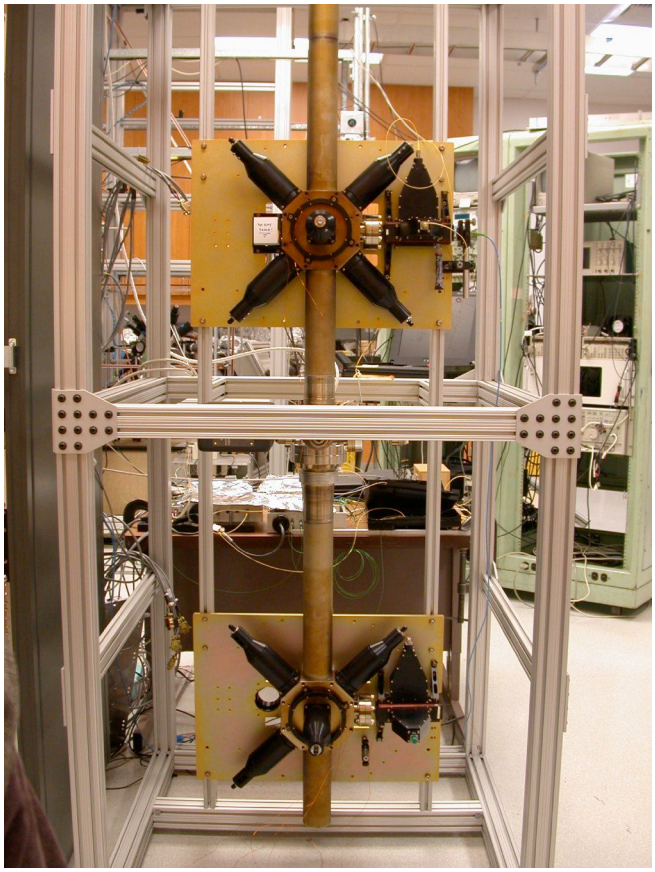

Fig. 4. The Atomic Physics Package during assembly, prior to installation of the magnetic shields The titanium/sapphire vacuum enclosure is shown mounted in the support frame along with various laser collimators and magnetic coils. The 2D-MOTs used as cold atom beam sources are visible to the right of the hexagonal UHV MOT chambers.

Sensitive operation of the gravity gradiometer requires the use of magnetic shielding to exclude external fields. We require the magnetic fields be less than 1 mG in the laser cooling region and on the order of a few μG or less in the interaction region. To achieve these conditions, we incorporate a cylindrical mu-metal shield around the interaction region and a single- or dual-layer mu-metal shield around the entire atom interferometer. The outer shields include a 70-mm diameter opening at the top and bottom for the vertical optical axis along the center and four additional 32×57 mm^2 openings for the support struts and cable routing. Finite element modeling indicates that external fields should be attenuated by $> 10^4$ throughout the interrogation region by the dual-layer shield geometry, and a factor of 200 for the single-layer geometry. The performance of the gradiometer with the single-layer outer shields is being evaluated in the laboratory, and the second outer layer of shielding may be retro-fitted later for operation in more severe environments, if necessary.

Fig. 5. One of two ECDL master laser modules in the Laser and Optics System.

B. *Laser system*

The laser and optics system (LOS) provides multiple laser beams needed for two 2-D MOTs, two UHV MOTs, and the atom interferometry beams (21 beams in total), each with individual control of frequency and/or intensity. A frequency-stabilized external cavity diode laser (ECDL) serves as a master laser, and a second ECDL is phase locked to the first. A single master laser module is shown in Fig. 5. Manipulation of the frequency offset for this phase lock provides the laser frequency agility required for laser trapping, sub-Doppler cooling, interferometry, and laser-induced fluorescence detection. The synthesis of this microwave reference frequency is discussed in the following section.

Eight injection-locked slave diode lasers are utilized for the individual MOT beams. Each of these slave laser modules (Fig. 6) produces up to 60 mW of fiber-coupled output power, which is divided with a fiber splitter and then expanded and collimated to produce a 24 mm diameter beam for the UHV MOTs. The power of each beam is monitored by using a beam sampler inside the custom collimators. Two more slave lasers are used to produce the trapping beams for the 2D-MOTs used as cold atom beam sources. These laser outputs are expanded and collimated to produce 13 mm × 44 mm elliptical beams. Additional slave lasers provide repumping beams for the UHV and 2D-MOTs, and to generate the Raman beams. A total of twelve injection-locked laser amplifiers are employed in the LOS, and yet the complete modular laser system can fit inside a 40 × 80 × 12 cm^3 volume.

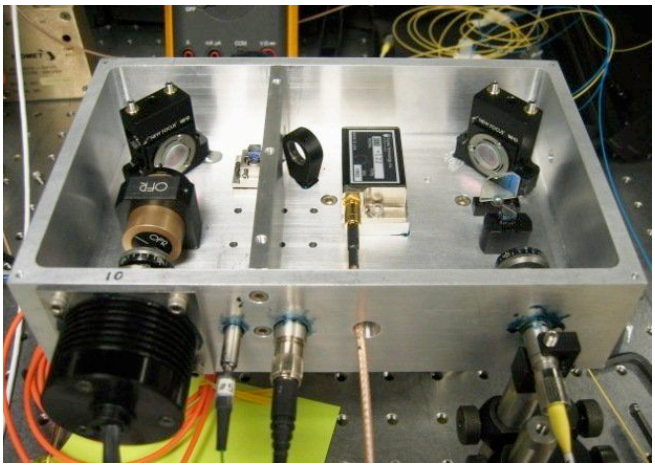

Fig. 6. A single slave laser amplifier module. A total of twelve laser amplifiers are employed in the Laser and Optics System.

C. *Frequency synthesis and control electronics*

Operation of the gravity gradiometer requires precise control of all laser frequencies and amplitudes, the applied magnetic fields, as well as generation of precise timing sequences for the optical and microwave pulses. Stand-alone operation in the mobile instrument additionally requires that the control system be able to acquire and maintain the phase and frequency stabilization locks over a range of temperatures and environmental conditions. These tasks are performed by a combination of software and hardware.

The laser frequency offset and phase difference are precisely controlled by a homemade phase-lock loop (PLL). The microwave reference frequency for the PLL is generated by a custom-designed microwave synthesizer based on a 9.2 GHz dielectric resonant oscillator (DRO) mixed with the output of a 120 MHz direct-digital synthesizer (DDS) chip. The DDS provides the frequency agility required for all laser-atom interactions, including atom cooling and trapping, launching atoms as in an atomic fountain, and the stimulated Raman pulses required for atom interferometry. The DDS architecture allows these frequency and phase states to be updated using a TTL trigger pulse at rates up to 1 kHz in order to synchronize the synthesizer event-states to the experimental sequence (see Fig. 7).

The precise timing required for the atom fountain operation and time-domain atom interferometry is provided by commercial multi-channel digital delay generators. The TTL timing pulse sequences modulate the rf drive levels for the laser system's various acousto-optic modulators (AOMs) to produce laser pulse sequences with better than 1 ns timing resolution over the 0.5 s measurement cycle, and less than 100 ns rise time for the individual optical pulses. Additional analog waveforms for laser intensity control are generated by a computer with multi-channel digital-to-analog boards. By employing voltage-controlled rf attenuators, the individual laser intensities can be precisely controlled

for each laser beam via these computer-generated waveforms.

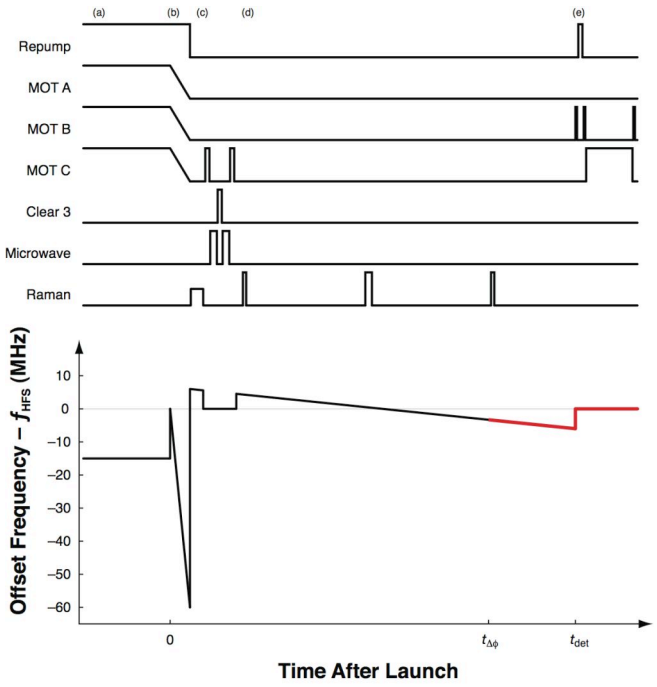

Fig. 7. Analog and digital voltage waveforms for laser and microwave intensity control (upper plots), and time-varying reference frequency for the experimental sequence (lower plot) where the labeled event-states are (a) atom collection, (b) atom launch, (c) velocity- and state-selection, (d) atom interferometry, and (e) quantum state detection.

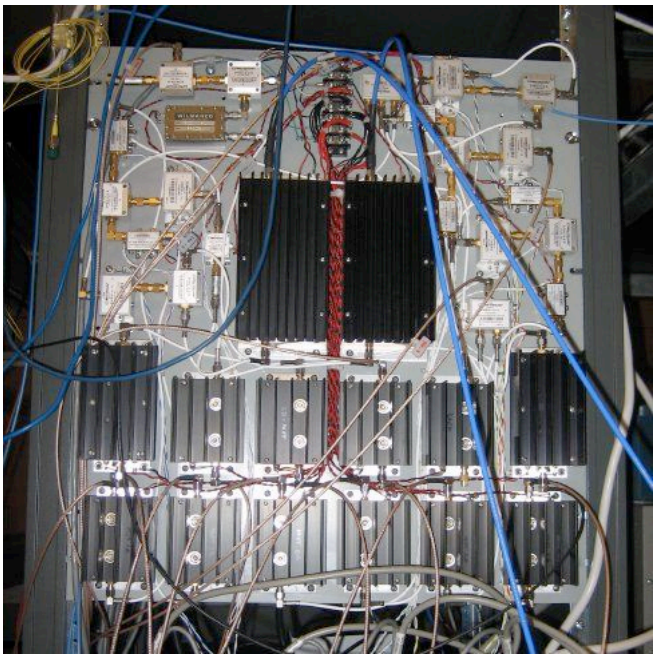

Fig. 8. Microwave and rf control electronics panel.

The control computer also generates voltages for controlling the multiple injection-locked amplifier laser currents and temperatures. We have demonstrated a robust algorithm for acquiring the injection locks for the twelve slave amplifier lasers, and the software is able to maintain these locks indefinitely for autonomous operation.

D. Phase feed-forward

One of the difficulties operating a gravity gradiometer on a mobile platform lies in adequately stabilizing the retro-mirror for the Raman laser beams. In order to facilitate operation in noisy environments, we have implemented a phase feed-forward scheme to detect and correct for vibrations by adjusting the phase of the Raman beams. This scheme can significantly reduce the amount of vibration isolation required and increase the dynamic range of the instrument. In the current implementation, an accelerometer on the mirror platform detects vibrations and feeds a correction signal to a phase modulator to electronically shift the phase of the microwave reference frequency for the laser phase lock (see Fig. 9). This produces a relative phase shift between the two Raman lasers which effectively cancels the phase shift resulting from the motion of the measurement platform. We have demonstrated greater than 70% reduction in atom interferometer phase noise due to spurious mechanical vibrations of Raman retro-mirror in our initial testing of this scheme.

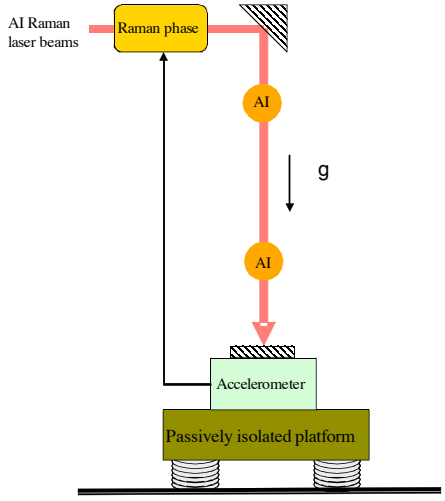

Fig. 9. Illustration of the phase feed-forward scheme

IV. Conclusions

We have reported on the design and development of a transportable gravity gradiometer, including the development and integration of the lasers, optics, electronics, and vacuum technologies for the various subsystems. This instrument represents an important step towards the development of an eventual space-flyable instrument. Such an in-

strument can achieve even greater sensitivity from operation in a microgravity environment, and will be able to apply the great sensitivity of quantum interference measurements to studies of Earth's gravity field from space.

ACKNOWLEDGEMENTS

We thank Lawrence Lim, Dmitry Strekalov, and Meirong Tu for technical assistance. This research was carried out at the Jet Propulsion Laboratory, California Institute of Technology, under a contract with the National Aeronautics and Space Administration. Reference herein to any specific commercial product, process, or service by trade name, trademark, manufacturer, or otherwise, does not constitute or imply its endorsement by the United States Government or the Jet Propulsion Laboratory, California Institute of Technology.

REFERENCES

[1] M. Kasevich and S. Chu, "Measurement of the gravitational acceleration of an atom with a light-pulse atom interferometer," Appl. Phys. B **54**, 321 (1992).
[2] A. Peters, K. Y. Chung, and Steven Chu, "High-precision gravity measurements using atom interferometry," Metrologia **38**, 25 (2001).
[3] F. Yver-Leduc, *et al*., "Reaching the quantum noise limit in a high sensitivity cold-atom inertial sensor," J. Opt. B **5**, S136 (2003).
[4] T. L. Gustavson, A. Landragin, and M. A. Kasevich, "Rotation sensing with a dual atom-interferometer Sagnac gyroscope," Class. Quantum Grav. **17**, 2385 (2000).
[5] J. M. McGuirk, G. T. Foster, J. B. Fixler, M. J. Snadden, and M. A. Kasevich, "Sensitive absolute-gravity gradiometry using atom interferometry," Phys. Rev. A **65**, 033608 (2002).
[6] N. Yu, J. M. Kohel, J. R. Kellogg, and L. Maleki, "Development of an atom-interferometer gravity gradiometer for gravity measurement from space," Appl. Phys. B **84**, 647 (2006).
[7] Ch. Reigber, *et al*., "A high quality global gravity field model from CHAMP GPS tracking data and accelerometry (EIGEN-1S)," Geophys. Res. Lett. **29**, 10.1029/2002GL015064 (2002); http://www.gfz-potsdam.de/pb1/op/champ/
[8] B. D. Tapley, S. Bettadpur, J. C. Ries, P. F. Thompson, and M. M. Watkins, "GRACE measurements of mass variability in the Earth system," Science 305, 503 (2004); http://www.csr.utexas.edu/grace/
[9] http://www.esa.int/export/esaLP/goce.html
[10] http://www.physics.umd.edu/GRE/SGGs.html
[11] Ch. J. Bordé, "Atomic interferometry with internal state labeling," Phys. Lett. A **140**, 10 (1989).
[12] M. Kasevich and S. Chu, "Atomic interferometry using stimulated Raman transitions," Phys. Rev. Lett. **67**, 181 (1991).
[13] D. B. Sullivan, *et al*., "PARCS: NASA's laser-cooled atomic clock in space," Adv. Space Res. **36,** 107 (2005).
[14] P. Lemonde, *et al*., "Test of a space cold atom clock prototype in the absence of gravity," IEEE Trans. Instrum. Meas. **48**, 512 (1999).
[15] http://sci.esa.int/hyper; Quantum Interferometer Einstein's Equivalence Principle Test (QuITE), a study funded by NASA's Fundamental Physics Program (2003).
[16] J. Ramirez-Serrano, N. Yu, J. M. Kohel, J. R. Kellogg, and L. Maleki, "Multistage two-dimensional magneto-optical trap as a compact cold atom beam source," Opt. Lett. **31**, 682 (2006).